SEISMIC PERFORMANCE TESTING OF PARTIALLY AND FULLY ANCHORED WOOD-FRAME SHEAR WALLS

Kevin B. D. White

Former Graduate Research Assistant
Department of Wood Science and Engineering
Oregon State University
Corvallis, OR 97331

*Thomas H. Miller**

Associate Professor
School of Civil and Construction Engineering
Oregon State University
Corvallis, OR 97331

Rakesh Gupta†

Professor
Department of Wood Science and Engineering
Oregon State University
Corvallis, OR 97331

(Received April 2009)

Abstract. Earthquake performance of wood-frame shear walls was evaluated by comparing fully and partially anchored walls under monotonic, cyclic, and earthquake loads and comparing with code measures. Suitability of monotonic and cyclic testing to predict seismic performance was examined. Earthquake tests were conducted on 2440-mm-square walls with Douglas-fir studs. Two oriented strandboard panels were fastened to the frame with two gypsum wallboard panels on the opposite side. Partially anchored walls had two anchor bolts on the sill plate. Fully anchored walls had hold-downs at the ends. Four time histories were tested: three subduction zone ground motions and a strike-slip fault, all scaled to the Seattle design level. For fully anchored walls, subduction zone tests had capacities, energy dissipation, and failure modes most similar to cyclic tests. Wall displacement at maximum load was underestimated by cyclic and overestimated by monotonic tests. For partially anchored walls, subduction zone and strike-slip earthquake tests had capacity, displacement at maximum load, initial stiffness, and ductility most similar to cyclic tests. Energy dissipation was most similar to monotonic tests, and failure modes were consistent with monotonic and cyclic tests. Partially anchored walls had lower capacity, displacement at maximum load, energy dissipation, and stiffness as compared with fully anchored walls.

Keywords: Seismic performance, wood-frame, shear wall, FEMA 356.

INTRODUCTION

Earthquakes and wind create lateral forces on buildings that are random and cyclic, reflecting the behavior of these environmental events. In California, the second most seismically active state (USGS 2004b), 99% of the residences are wood-framed construction, whereas throughout the United States, wood structures are 80 – 90% of the total (Malik 1995). Shear walls are the most common vertical lateral force-resisting element in light-frame construction, and in 1997, over 90% of US residences used them as the primary lateral load-resisting system (PCA 1997). Therefore, their ability to adequately resist random and cyclic lateral forces is critical to the safety of the inhabitants and to the soundness of our residential infrastructure.

Design values for wood shear walls are based on static tests. Static (or monotonic) tests do not

* Corresponding author: Thomas.Miller@oregonstate.edu
† SWST member

Wood and Fiber Science, 41(4), 2009, pp. 396–413

apply either cyclic or random load reversals that occur during an earthquake or wind event. Static tests push the wall to failure by loading the top in one direction at a constant rate of displacement. This loading discrepancy was not believed to be significant until the 1994 Northridge earthquake in southern California. Not only was this the most costly earthquake in US history (estimates up to $40 billion), but it killed 60 people, injured more than 7000, and damaged over 40,000 homes (USGS 2004a). Since the occurrence of this natural disaster, substantial research has been directed toward the development of cyclic-testing protocols that are more representative of the loading seen during earthquakes. Almost all of this research has been focused on mitigating the damage associated with strike-slip earthquakes—like Northridge, that are common to California—through development of appropriate cyclic-testing protocols. However, the major fault mechanism in the Pacific Northwest is a subduction zone (Cascadia Subduction Zone), not strike-slip. Historically speaking, subduction-zone earthquakes are more infrequent than strike-slip earthquakes, yet have the potential to be of larger magnitude and longer duration from the buildup of energy over a long period of time and the potential for a large fracture area.

Most shear wall testing has been conducted on walls with hold-downs and anchor bolts (fully anchored walls) despite the International Residential Code (IRC) (ICC 2000) and its predecessors allowing for lateral resistance from walls with only anchor bolts (partially anchored walls). Very little research has been directed toward assessing the performance of partially anchored walls under monotonic, cyclic, or earthquake loads.

Thus, this study has the following objectives:

1. Evaluate and compare the performance of fully and partially anchored walls under monotonic, cyclic, and earthquake loads;
2. Compare wall performance under earthquake loads with that from standardized monotonic and cyclic tests; and
3. Evaluate dynamic wall performance with respect to code performance measures.

LITERATURE REVIEW

There have been several cyclic and shake table studies conducted to determine the performance of wood stud shear walls. Filiatrault and Foschi (1991) compared the performance of conventionally constructed walls with those with nails and adhesive. Test protocols included static and earthquake time histories from San Fernando in1971, El Centro in 1940, and Romania in 1977. Walls with adhesive remained elastic under moderate (design) and large earthquake conditions, but conventionally constructed walls behaved inelastically for the design level earthquake and were near total collapse for large earthquakes. Dolan and Madsen (1992) performed shake table testing of light-frame wood shear walls, examining performance in the 1952 Kern County and 1971 San Fernando earthquakes both experimentally and analytically. Several sheathing–nailing combinations were subjected to various amplitudes of each earthquake. Karacabeyli and Ceccotti (1998) tested walls using static, cyclic, and pseudodynamic procedures. Failure modes of nail fatigue, nail pullthrough, nail withdrawal, and nail tearout were observed and were dependent on test protocol. Nail fatigue was common to protocols with high energy demands. The basis for design unit shears was suggested to be the first envelope from cyclic tests or the monotonic curve. Dinehart and Shenton (1998) conducted static and Sequential Phased Displacement (SPD) shear wall tests. Because of the increased cycling of the SPD tests, static tests had a slightly larger wall capacity and a much greater displacement at maximum load that corresponded to a 40% higher ductility. Nail fatigue and withdrawal were common to the SPD test; this was very different from that of static testing.

Yamaguchi et al (2000) ran monotonic and cyclic tests with various loading rates, pseudodynamic tests, and El Centro shake table tests.

Tests with more load cycling and high amplitudes corresponded to greater postpeak strength degradation. The fast-reversed cyclic test had results closest to shake-table tests. Pseudodynamic tests had similar amplitudes and load cycles to shake-table testing but had results that were the most different. McMullin and Merrick (2000) tested walls sheathed on both sides with oriented strandboard (OSB), 3-ply plywood, 4-ply plywood, or gypsum wallboard (GWB) using force-controlled cyclic tests. The stiffness of gypsum wallboard was found to be greater than that of plywood and OSB, thereby attracting significant load during the initial stages of an earthquake, leading to subsequent damage.

Salenikovich and Dolan (2003a, 2003b) tested walls with various aspect ratios and overturning restraints both statically and cyclically. Wall capacity and corresponding displacement were 13 and 30% greater, respectively, for walls tested monotonically and having aspect ratios less than or equal to 2:1, whereas wall ductility and wall stiffness were about the same as a result of the two protocols. Gatto and Uang (2003) ran tests on 2440-mm-square walls sheathed with plywood or OSB using static, CUREE standard (Krawinkler et al 2001), ISO (1998), SPD, and CUREE near-fault protocols (Krawinkler et al 2001). Tests with large numbers of cycles and equal amplitude cycle groups appeared to be the most rigorous. The CUREE standard protocol had failure modes consistent with seismic behavior and therefore was suggested to be a standard procedure for future wood-framed testing.

The majority of the literature has been focused on testing engineered walls with hold-downs (Pardoen et al 2000; Uang 2001) despite the IRC allowing shear resistance from walls not having them. However, Ni and Karacabeyli (2002) studied the performance of shear walls anchored with hold-downs, without hold-downs, and with dead-load and no hold-downs. Static and the reverse cycling ISO (1998) loading protocols were used. Maximum load and corresponding displacement of walls without hold-downs or vertical load was 50% that of walls with hold-downs and no vertical load. Ni and Karacabeyli's (2002) testing of walls without hold-downs used inconsistent wall configurations per the brace panel construction specified in the IRC.

Limitations of the research discussed relative to this project include:

1. Shake-table studies used strike-slip earthquake time histories. The duration, frequency content, and magnitude of subduction zone earthquakes may cause a different structural response.
2. Limited research has focused on the performance of walls without hold-downs and, furthermore, did not use wall configurations that are consistent with those specified in the IRC. This study quantifies performance of walls without hold-downs that have proper configuration per the IRC—as is common in residential construction—and does so under earthquake loading.

As a result of the 1994 Northridge earthquake, the City of Los Angeles/UC Irvine implemented a shear wall test program (City of Los Angeles/UC Irvine 2001). From this program, recommendations were made to reduce design shear values based on monotonic tests similar to Dinehart and Shenton (1998), in which a 25% reduction was recommended as a result of a reduction in load between the first and fourth cycles from cyclic testing using the SPD protocol. However, to the contrary, Cobeen et al (2004) stated that there is currently no evidence to support a reduction in design loads. Because performance comparisons of shake-table tests with monotonic and cyclic tests have been conducted here, this project contributes to this discussion.

MATERIALS AND METHODS

Wall Specimens

Shear wall test specimens were built in accordance with prescribed braced panel construction in the 2000 IRC (ICC 2000). All tests

were conducted on identical 2440- × 2440-mm walls constructed using Standard & Better 38- × 89-mm kiln-dried Douglas-fir framing as shown in Fig 1. Framing studs were spaced at 610 mm on center and connected to the sill plate and first top plate using two 16d (4.11 × 88.9 mm) common nails per connection driven through the plates and into the end grain of the stud. A second top plate was connected to the first top plate using 16d nails at 610 mm on center. Walls were sheathed using two 1220- × 2440- × 11.1-mm OSB panels attached vertically to the wall frame while spaced 3.2 mm apart. The 24/16 APA-rated OSB panels were connected to the wall frame using 8d (3.33 × 63.5 mm) common nails spaced 152 mm on center along the panel edges and 305 mm along intermediate studs. Walls were additionally sheathed with two 1220- × 2440- × 12.7-mm GWB panels installed vertically on the face opposite the OSB structural panels. GWB panels were attached to the framing with bugle-head coarse wallboard screws (2.31 × 41.3 mm) spaced 305 mm on center along the panel edges and intermediate studs. Sheathing-to-framing connections were not staggered. Double end studs were required for walls with hold-downs and were connected together using 16d nails at 305 mm on center. Framing and sheathing nails were full round head, strip cartridge, and smooth

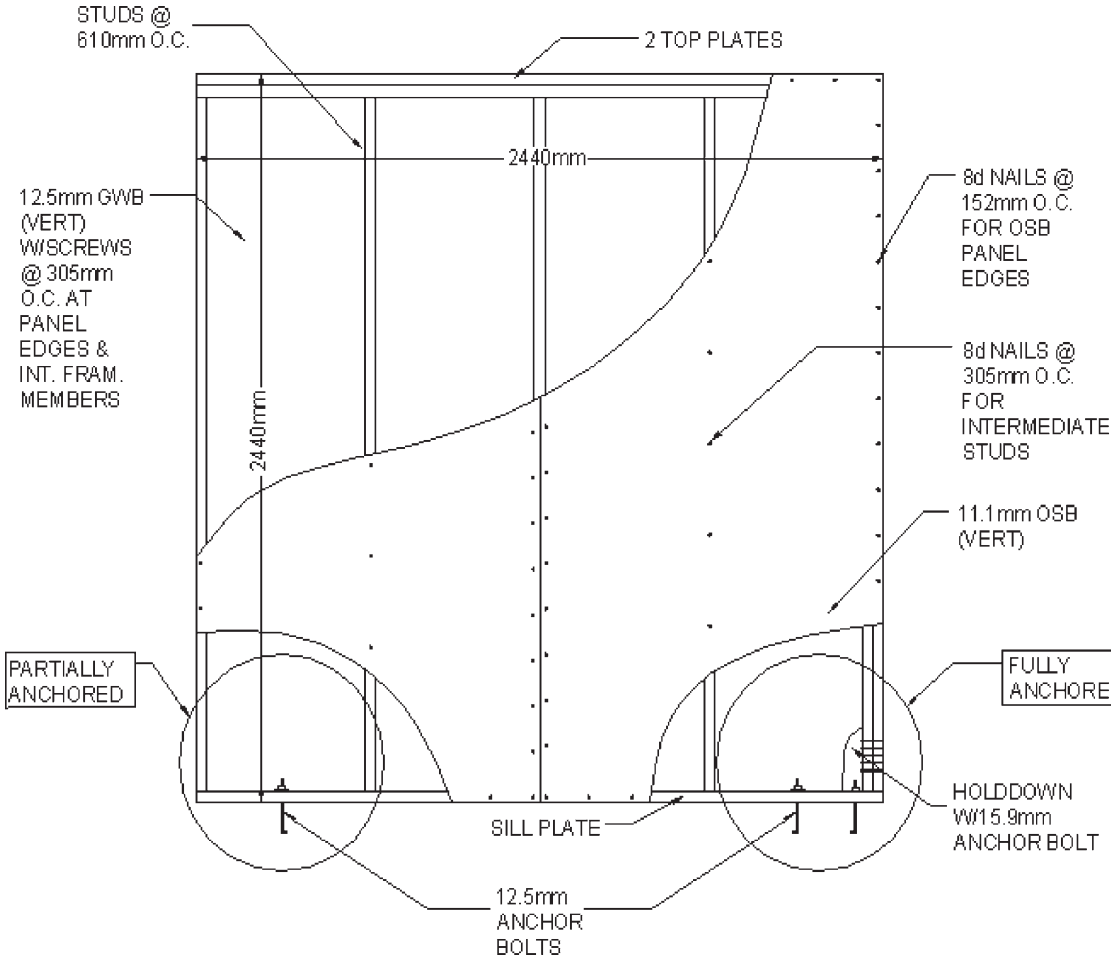

Figure 1. Schematic of shear wall test specimen.

shank SENCO® nails driven using a pneumatically driven nail gun.

Wall Anchorage

Wall specimens were connected to the testing frame using one of two anchorage methods (Fig 1). The most basic is per the IRC for brace-panel construction using structural panel sheathing. This does not require hold-downs; it assumes proper connection to the foundation is provided by 12.5-mm anchor bolts installed at a minimum of 1829 mm on center. These "partially anchored" walls were attached to the test frame using 12.7-mm A307 anchor bolts placed 305 mm inward from each end of the wall. Fully anchored walls added two SIMPSON Strong-Tie® PHD-2 hold-downs installed to double end studs. Each hold-down was attached to the test frame with a 15.9-mm Grade 5 bolt.

Testing Frame and Equipment

A schematic of the test frame used for the earthquake and monotonic tests is shown in Fig 2. The test frame consists of a 102- × 152- × 10-mm steel beam on linear bearings, one at each end of the beam. Two 51-mm solid steel rods rigidly attached to the strong floor of the laboratory were guides for the bearings. A 4.45-kN servo-controlled hydraulic actuator capable of 153-mm stroke was used to drive the steel load beam horizontally in one dimension to simulate ground motions. Walls were connected to the moveable steel load beam, essentially serving as a foundation.

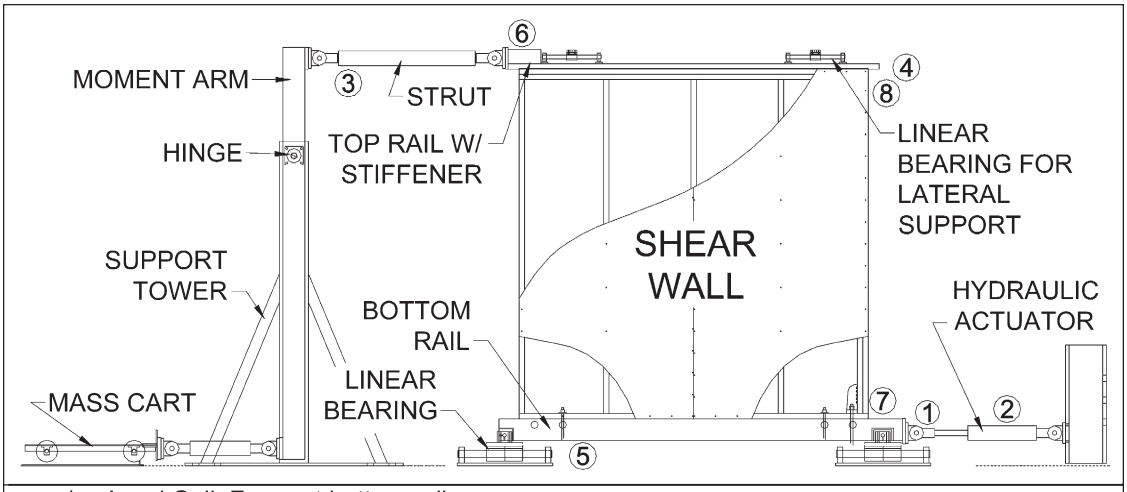

1. Load Cell: Force at bottom rail
2. Internal Linearly Variable Differential Transformer (LVDT): Bottom rail displacement
3. Load Cell: Force at top rail
4. String Potentiometer: Top rail displacement
5. Accelerometer: Bottom rail acceleration
6. Accelerometer: Top rail acceleration
7. LVDT: Stud to bottom rail uplift
8. LVDT: Stud to top rail separation

Figure 2. Schematic of dynamic test frame (Seaders et al 2009b).

Shear walls in buildings laterally support the mass of all components tributary to them from the structure above. Here a 4543-kg tributary mass was used for a typical shear wall in a 140-m^2 residential home. For safety, seismic mass was placed on a steel cart that rolled on the floor and was connected to the top of the wall. The cart rested on steel tracks rigidly attached to the strong floor of the laboratory, and it was also connected to the bottom end of the moment arm by means of a steel rod pinned at both ends with 25.4-mm spherical rod ends. The steel channel bolted to the top of the walls was laterally braced to a strong wall in the laboratory through a series of steel struts. This limited movement of the top of the wall to the one dimension in which the wall was being driven by the hydraulic actuator.

Data Collection

Two load cells were used to measure wall forces during testing (Fig 2). The first was a 90-kN load cell connected in line with the hydraulic actuator and the steel beam serving as the foundation for the walls. This load cell measured the force at the bottom of the wall required to achieve the desired ground motion and move the seismic mass. The second load cell was 55.6 kN rated and in line between the top of the steel moment arm and the steel channel bolted to the top of the wall, measuring force at the top of the wall. Load beam displacement was monitored by a sensor built into the hydraulic actuator measuring cylinder position. Displacement at the top of the wall was monitored using a string potentiometer between the strong wall of the laboratory and the double top plate.

Uplift displacements of the double top plate with respect to the end stud of the wall and the end stud with respect to the foundation were also monitored. For the double top plate, this was achieved by mounting a linearly variable differential transducer (LVDT) on the end stud and monitoring its displacement with respect to the steel channel bolted to the top of the wall (Fig 2). Likewise, an LVDT was mounted on the end stud and its displacement with respect to the foundation was monitored for bottom uplift. Uplift was recorded from one side of the wall only to ensure that a high-frequency data-sampling rate could be maintained, necessary to embody the dynamic response of the wall. If needed, the uplift response of the opposite end of the wall could be determined as a function of drift and the measured uplift response.

Earthquake Time Histories

Selection. Selection of earthquake ground motions was based on many factors. A primary goal of this study was to determine the response of shear walls when subjected to ground motions expected in the Pacific Northwest affected by the Cascadia Subduction Zone. Thus, ground motions were to be high amplitude and long duration, typical of subduction zones. The SAC Steel Project (Somerville et al 1997) contained a suite of ground motions meeting these criteria including those for Seattle at: 1) 2% probability of exceedance in 50 yr; and 2) 10% probability of exceedance in 50 yr. In addition to several subduction zone ground motions, a strike-slip fault mechanism was also chosen (Table 1). Because structural response is dependent on the frequency content and acceleration of the earthquake time history, additional ground motion selection criteria were: 1) collectively, the ground motions cover a broad range of frequencies (or periods) (1 – 10 Hz or 0.1 – 1 s); and 2) the time histories fall within the $\pm$79-mm displacement limitation of the available testing equipment.

Scaling. The acceleration-time histories obtained from the SAC Steel Project had been scaled from the original (or actual) ground motions to match a design spectrum at periods of interest for steel structures. Because steel structures generally have a longer period of vibration than wood frame structures, the time histories needed to be rescaled to the appropriate level for a typical wood building in Seattle. To scale the time histories appropriately for this study, a design response spectrum was generated according to FEMA 356 (FEMA 2000) at the 10% probability of exceedance in a 50-yr

Table 1. *Description of selected earthquakes.*

Characteristic	SE03	SE07	SE13	SE19
Earthquake name	1984 Morgan Hill	1949 Olympia	1965 Seattle	1985 Valparaiso
Recording location	Gilroy, CA	Seattle Army Base	Federal Office Building, Seattle	Vina del Mar, Chile
Time	24 Apr. 1984	13 Apr. 1949	29 Apr. 1965	3 Mar. 1985
Mechanism	Strike-slip	Subduction intraplate	Subduction intraplate	Subduction interface
Dist from epicenter (km)	15	80	61	42
Magnitude (M_w)	6.2	6.5	7.1	8.0
Site (soil condition)	S_d (soil)	S_d (soil)	S_d (soil)	S_d (soil)
Scale factor (Seattle/original)	1.654	5.125	3.998	0.962
Peak accel (m/s^2)	2.29	2.73	3.06	3.03
Peak vel (mm/s)	198	346	365	370
Peak Displ (mm)	50	72	63	55
Duration (s)	60.00	66.72	74.16	100.05
Time step (s)	0.020	0.020	0.020	0.025

level for downtown Seattle using a type "D" soil (S_d) classification [stiff soil with 183 m/s < shear wave velocity of soil (v_s) $\leq$ 366 m/s; used as the default site class per FEMA 356 1.6.1.4.2]. Because most wood structures are 3 – 9 m tall, they have natural periods of vibration between 0.1 – 0.3 s according to the empirical equation provided by FEMA 356:

$$T = C_t \cdot h_n^{\beta} \quad (1)$$

where T is the fundamental period of vibration (s), C_t is 0.146 for wood buildings, h_n is the roof height (m), and β is given as 0.75. Using this information, the average spectral acceleration within the 0.1 – 0.3-s target-period range (shown in Fig 3) was determined for each of the time histories. Earthquake response spectra and corresponding time histories were then scaled (to the Seattle Design Level; 10% probability of exceedance in 50 yr) by the ratio of the average spectral acceleration from the FEMA 356 Seattle Design Level response spectrum to the average spectral acceleration from the earthquake response spectrum in the 0.1 – 0.3-s period range.

Data Analysis

Backbone analysis. Analyzing the backbone curve provides a means to compare results from monotonic, cyclic, and earthquake testing. Each earthquake test yields a backbone curve with two segments, one segment for positive wall drift and the other for negative wall drift. Backbone curves were constructed, up to maximum load (P_{max}) for both positive and negative drift, by drawing a line between points of successively increasing peak loads on hysteretic cycles. Beyond P_{max}, backbone curves were constructed by drawing a line from P_{max} to the successively smaller peak loads on hysteretic cycles. Backbone curves were terminated at the peak load on the hysteretic cycle that contained the largest drift. Wall failure, as defined here, occurred at $0.8P_{max}$ postpeak.

Because an earthquake test yields a backbone curve with two segments, an average value for an earthquake test protocol was obtained by: 1) averaging absolute values reported for a given parameter from the positive and negative backbone curve segments for an individual test; and then 2) combining this value with corresponding values from the remaining tests having the same earthquake protocol and wall anchorage and determining the mean unless otherwise noted. In general, the backbone analysis is similar to that recommended in ASTM E 2126 (ASTM 2001).

Period estimates and calculations. Wall period becomes longer during an earthquake test as a result of stiffness degradation from

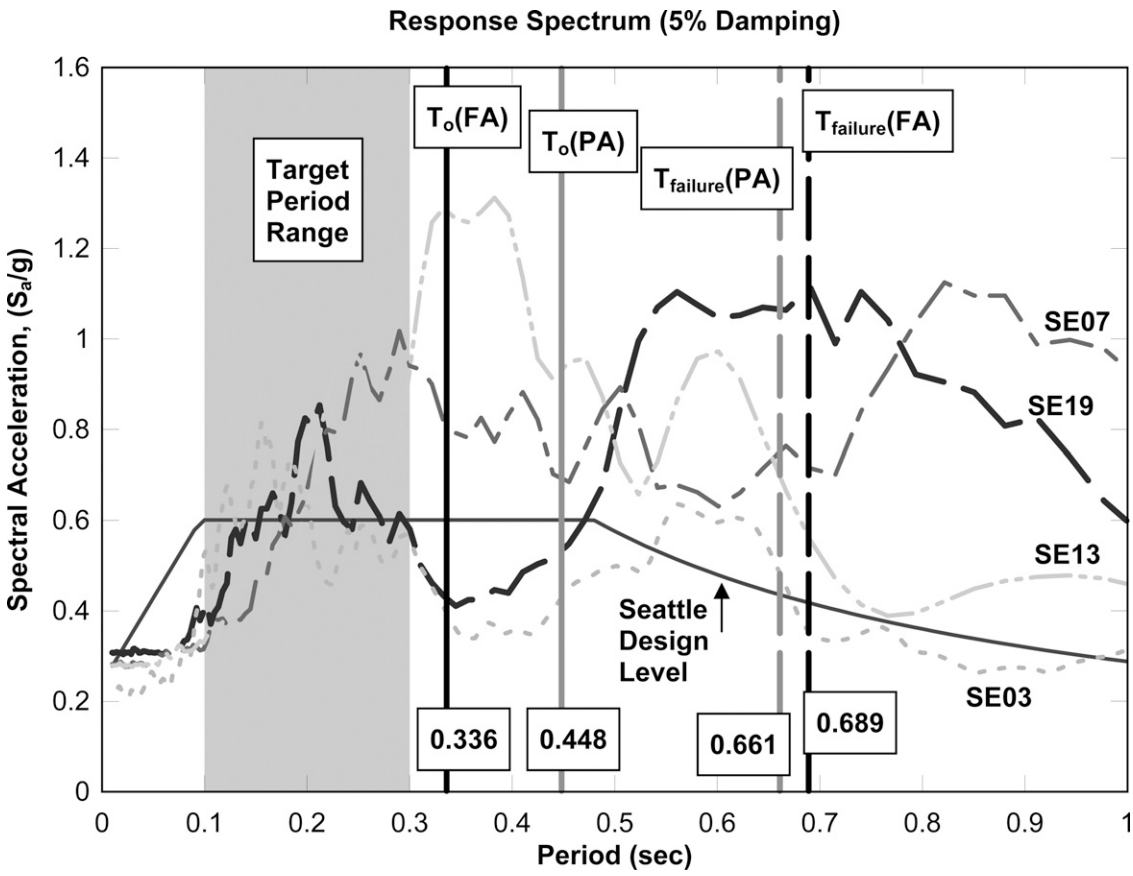

Figure 3. Comparison of average wall periods and scaled (to Seattle Design Level) earthquake response spectra.

damage accumulation. Fundamental period (T_o) and period at maximum load ($T_{failure}$) were calculated for each test:

$$T = 2 \cdot \pi \cdot \left(\sqrt{\text{mass/stiffness}}\right) \qquad (2)$$

Fundamental period (T_o) was calculated using the initial stiffness (k_e) defined as the slope of the backbone curve up to $0.4P_{max}$ ($k_e = 0.4P_{max}/\Delta_e$). The failure period ($T_{failure}$) was calculated using the secant stiffness (k_{secant}), defined as the slope of the backbone curve up to P_{max} (P_{max}/Δ_{max}). Comparisons of the fundamental period calculated with Eq 2 and the FEMA 356 empirical formula (Eq 1) were performed.

Cumulative drift. Cumulative drift ($\Delta_{cumulative}$) is a parameter developed by Seaders et al (2009b). It is the summation of the absolute value of the change in drift for each step (Eq 3). Therefore, a wall that accumulates a significant amount of damage and has a subsequent loss of stiffness will generally exhibit a high level of $\Delta_{cumulative}$. For this reason, $\Delta_{cumulative}$ will be used to indicate the severity of loading conditions as a result of particular earthquake tests. In addition, $\Delta_{cumulative}$ is an important measure because the relative motion of stories within a building (interstory drift) is a primary source (and indication) of damage and stiffness degradation.

$$\Delta cumulative = \sum_i \left(|\text{Drift}_i - \text{Drift}_{i-1}|\right) \qquad (3)$$

Because the change in relative displacement is recorded at each time step, cumulative drift can be summed over any interval. Cumulative drift

up to and including the drift cycle containing maximum load ($\Delta_{cumulative\text{-}Pmax}$) is also of interest; it provides insight into the demands on the wall up to ultimate loading conditions.

Average spectral acceleration. T_o and $T_{failure}$ of a wall are the two extreme values characterizing the critical region containing the shift (increase) in wall period that occurs up to maximum loading during an earthquake as a result of wall stiffness degradation. A response spectrum with large accelerations within the critical region is more likely to cause damage. Average spectral acceleration provides a method to evaluate the levels of acceleration in the critical region and is calculated by summing the values of spectral acceleration (S_a) in the critical region and dividing by the number of observations.

$$\text{Average spectral acceleration} = \sum_{T_o}^{T_f} S_{a_i}/n \tag{4}$$

where n is number of observations in the interval. Wall stiffness is different for fully and partially anchored walls; they have different critical regions.

FEMA 356 m-factor analysis. Wood shear walls are deformation-controlled elements because they exhibit significant inelastic behavior before strength loss, and thus, their ductility can be evaluated using m-factors per FEMA 356 (FEMA 2000). The m-factor is for structural components, not the entire lateral force resisting system. The acceptance criteria for deformation-controlled (ie ductile) elements as defined in FEMA 356 is:

$$m \cdot \kappa \cdot Q_{CE} \geq Q_{UD} \tag{5}$$

where m is the modification factor that indicates the available ductility, κ is a knowledge factor to account for uncertainty in the analysis of existing structures, Q_{CE} is the expected element strength at the deformation level being considered, and Q_{UD} is the deformation-controlled design action resulting from earthquake and gravity forces.

An m-factor analysis involves creating idealized load-displacement curves drawn in conjunction with corresponding backbone curves. An idealized curve is constructed by drawing a linear segment from the origin through the point at $0.6P_{max}$ in the elastic region on the backbone curve. Next, an additional linear segment is drawn such that the areas under the idealized curve and backbone curves up to failure are equal.

Individual m-factors for each test were determined by drift ratios: the ratio of drift at the desired structural performance level to the drift at the yield point on the idealized curve. Collapse prevention (CP) drift is that corresponding to the failure point of the idealized curve. Life safety (LS) and immediate occupancy (IO) levels are 0.75 and 0.5025 of the collapse prevention drift, respectively.

Wall failure modes. Posttest wall evaluation was conducted to determine the overall condition of test specimens by recording failure location and type for the primary elements of the wall (studs, double top plate and bottom plate, sheathing, and fasteners). Earthquake tests exhibited several failure modes; each involved failure of fasteners connecting the sheathing and the framing together. Fastener failure modes were classified into five general categories: 1) edge breakout from the nails and or GWB screws; 2) nail pull-through; 3) nail withdrawal; 4) localized crushing of the gypsum wallboard; and 5) fracture of screws attaching the GWB.

RESULTS AND DISCUSSION

Performance Differences of Fully and Partially Anchored Shear Walls

Based on the backbone curves, all fully and partially anchored subduction zone earthquake tests resulted in ultimate loading conditions and caused significant damage. In addition, these tests caused large levels of cumulative drift ($\Delta_{cumulative}$) and total energy dissipation (E_{total}), parameters that indicate loading severity (Table 2). For fully and partially anchored walls tested with the SE03 strike-slip ground motion,

Table 2. *Selected parameters from earthquake tests.*

	Fully anchored				Partially anchored		
	Strike-slip	Subduction zone			Subduction zone		
Parameter	SE03	SE07	SE13[a]	SE19	SE07	SE13[a]	SE19
P_{max} (kN)	16.31[b]	19.69	23.38	21.43	8.99	8.75	8.35
$\Delta_{cumulative}$ (mm)	1002	4907	2649	5428	4688	2435	4850
$\Delta_{cumulative\text{-}Pmax}$ (mm)	432	1846	559	471	1420	389	463
E_{total}[c] (J)	2177	12,163	3882	9143	3698	1798	3538
E_{Pmax}[d] (J)	1463	6665	2405	2608	790	665	747
$\Delta_{cumulative\text{-}Pmax}$ (mm)	432	1846	559	471	1420	389	463
cycles to P_{max}[e]	18	37	19	34	21	15	29
U_{max} (mm)	2.4	8.5	8.1	6.3	61.2	50.4	101.0

[a] Conducted by Seaders et al (2009b).
[b] Maximum observed value. Walls were not loaded to their full capacity.
[c] Total energy dissipated during the entire duration of earthquake testing.
[d] Total energy dissipated up to and including hysteretic cycle containing P_{max}.
[e] Number of load reversing cycles up to and including cycle containing P_{max}.

the $\Delta_{cumulative}$ and E_{total} levels indicate the loading conditions were less severe than subduction zone tests.

SE03 strike-slip earthquake test performance. The SE03-FA backbone curve did not exhibit postpeak behavior or significant inelastic deformations. As a result, this test caused much lower levels of $\Delta_{cumulative}$ and E_{total} (Table 2), parameters that indicate the severity of loading, and exhibited much less damage than corresponding subduction zone earthquake tests. In general, damage consisted of minor nail withdrawal from the frame and localized GWB crushing around screws attaching it to the frame.

Like corresponding subduction zone earthquake tests, the partially anchored SE03 strike-slip earthquake test attained ultimate loading and exhibited nonlinear performance. Overall, damage from this test was similar to that of corresponding subduction zone earthquake tests. Damage included localized GWB crushing, minor nail withdrawal from the framing, and edge breakout of sheathing to sill plate screw and nail fasteners (although less often than for subduction zone earthquake tests). In general, damage from the SE03 strike-slip ground motion was similar to that of subduction zone ground motions for partially anchored walls and much less severe for fully anchored walls.

Figure 3 provides an explanation of the performance differences of SE03 tests and the corresponding subduction zone tests for both fully and partially anchored walls. In particular, for fully and partially anchored walls, the critical regions that are bounded by T_o and $T_{failure}$, respectively, both fell within the lower acceleration region of the SE03 response spectrum. In comparison, subduction zone ground motions exhibited larger accelerations in both of these critical regions. For fully anchored walls, average spectral acceleration within the critical region for SE03 was 36, 49, and 40% below that of SE07, SE13, and SE19, respectively. Thus, it seems reasonable that fully anchored SE03 tests resulted in less damage and lower levels of loading compared with the corresponding subduction zone tests.

For partially anchored walls, the average spectral acceleration within the critical region for SE03 was 25, 36, and 42% below that of SE07, SE13, and SE19, respectively. However, because the capacity of partially anchored walls is about 40% of that of fully anchored walls, the differences in average spectral acceleration did not result in large differences in loading and damage as was the case for fully anchored walls.

Observed failure modes from subduction zone earthquake tests. In general, subduction zone earthquake tests on partially anchored walls exhibited failure modes of screw and nail

edge breakout along the sill plate. This failure mode was also common to corresponding monotonic and cyclic tests from Seaders et al (2009a). Once these connections failed, the walls exhibited little shear capacity and the top moved very little (compared with before the failure of these connections) as the bottom of the wall tracked the time history. This behavior resulted in partially anchored walls having large levels of $\Delta_{cumulative}$ after maximum loading conditions (note the difference in $\Delta_{cumulative}$ and $\Delta_{cumulative\text{-}Pmax}$ as shown in Table 2). In a few instances, sheathing to sill plate damage was so extensive the wall was almost completely detached from the sill plate. Other damage was minimal. Because damage to partially anchored walls was almost entirely along the sill plate, the three subduction zone earthquakes collectively had low variability in damage (with respect to severity, abundance, and location).

Fully anchored subduction zone earthquake tests had more damage than partially anchored walls as a result of the stiff hold-down connections to the foundation. This connection resulted in the sheathing panels undergoing rigid body rotation as the wall was racked. Fully anchored walls utilized a greater number of connections between the sheathing and framing members, and thus damage was distributed throughout the wall more evenly than for partially anchored walls, and there was higher variability in damage. Failure modes from fully anchored subduction zone earthquake tests consisted of: 1) GWB and OSB edge breakout; 2) nails pulling through the sheathing; 3) nails withdrawing from the frame; 4) screws causing localized crushing in the GWB; and/or 5) screw fracture.

In general, for fully anchored walls, screw fracture and nail withdrawal were more prevalent in subduction zone earthquake tests with a large number of reverse loading cycles. Screw fracture was common along the sill plate and vertical studs along the GWB panel edges and generally the damage was so extensive that the GWB panels lost their lateral load carrying capacity. Nail withdrawal from the framing was common to the vertical edges of the OSB sheathing and to the outer 610 mm of horizontal OSB panel edges. However, the most extensive damage to the OSB sheathing was at the panel edges (horizontal and vertical) located within the middle 1220 mm of the wall as a result of significant nail withdrawal, nail pullthrough, or OSB or GWB edge breakout. This damage often resulted in a small gap between the OSB sheathing and the wall framing along the center stud of the wall on test completion. In general, damage from fully anchored subduction zone tests corresponds best with the collapse prevention structural performance level for wood stud walls in Table C1-3 of FEMA 356 (FEMA 2000).

In general, for fully anchored walls, the SE19 and SE07 tests caused the most damage. SE13 conducted by Seaders et al (2009b) caused the least amount of damage among fully anchored subduction zone earthquake tests; however, it caused more than the corresponding SE03 test. Fully anchored monotonic tests from Seaders et al (2009b) primarily consisted of nail pullthrough and localized crushing of the GWB. Nail withdrawal and screw fracture, common to the subduction zone earthquake tests, also occurred during the cyclic tests from Seaders et al (2009b). Therefore, failure modes of fully anchored subduction zone earthquake tests were most similar to cyclic tests rather than monotonic tests.

Load paths. Fully and partially anchored walls exhibited different load paths. For partially anchored walls, the path for overturning forces to be transmitted into the foundation was through the sheathing to sill plate nail and screw connections, and wall performance was limited by the edge breakout capacity of these connections. Once these fasteners broke through the sheathing edge, partially anchored walls lost shear capacity, had poor drift performance, and had large uplift between the sill plate and end studs (U_{max}) (Table 2). When hold-downs are installed, the sheathing transfers overturning forces into the wall end studs and subsequently into the foundation through the hold-downs. Compared with partially anchored walls, the

fully anchored wall load path engages more fasteners because the transfer of load from sheathing to end studs is more evenly distributed throughout the wall. In this study, the result of this was that fully anchored walls had: 1) damage that was more evenly distributed throughout the wall (rather than at the sill plate); 2) favorable wall performance with respect to P_{max}, Δ_{max}, E, and k_e ; and 3) less wall uplift by providing a stiff and durable attachment between the frame and the foundation (Table 2).

As a result of the differing load paths of fully and partially anchored walls, the following correlations were only applicable to fully anchored walls. This is because the capacity of partially anchored walls appeared to be limited by the edge breakout strength of the sheathing to sill plate nail and screw fasteners. The first trend relates wall capacity (P_{max}) with energy dissipation up to and including the load cycle containing P_{max} (E_{Pmax}). SE07 and SE19 tests both had about the same number of reverse load cycles up to P_{max} (cycles to P_{max}); however, SE07 exhibited a 9% lower P_{max} (Table 2). This could be a result of SE07 causing cumulative drift up to maximum loading ($\Delta_{cumulative\text{-}Pmax}$) and subsequent energy dissipation (E_{Pmax}) levels that were 292 and 156% larger than SE19, respectively. Therefore, it appears that fully anchored tests with high levels of E_{Pmax} result in lower P_{max}. This trend agrees with the findings of Karacabeyli and Ceccotti (1998).

The second trend relates P_{max} with cycles to P_{max}. Although SE13 and SE19 tests had about the same E_{Pmax}, SE19 had a wall capacity of 21.43 kN, about 10% less than SE13 (23.38 kN) (Table 2). In addition, SE19 had approximately twice as many load cycles to P_{max} and the most severe and extensive fastener damage among all the fully anchored earthquake tests.

Dinehart and Shenton (1998), He et al (1998), and Karacabeyli and Ceccotti (1998) found that test protocols with more load reversing cycles cause more fastener fractures. When fasteners fracture in a wall, the load is transferred to other fasteners that are still intact, and the remaining fasteners are more likely to be overstressed as well. Thus, a fracture serves as a catalyst for additional fastener fracture or damage and also causes less favorable wall performance because wood shear wall performance is dependent on the number of sheathing to frame fasteners. Thus, for fully anchored walls, it appears that the SE19 earthquake test likely had a smaller P_{max} than SE13 because of greater cycles to P_{max}.

Performance differences based on backbone curves. On average, for subduction zone earthquake tests, fully anchored walls exhibited P_{max}, Δ_{max}, E, and k_e approximately 2.5, 2.8, 4.4, and 1.6 times that of partially anchored walls, respectively (Table 5). For these parameters, this significant difference in performance is a result of the differing load paths previously discussed.

Statistical tests (Table 3) comparing the mean performance of fully and partially SE19 tests

Table 3. *Statistical comparison of fully and partially anchored walls tested with the SE19 ground motion.*

	SE19-FA[a] (n = 8)		SE19-PA[a] (n = 8)		P values: FA vs PA (SE19)	
					F-test[b]: variance test	T-test[b]: mean test
Parameter	Avg. (μ_1)	Std. dev. (σ_1)	Avg. (μ_2)	Std. dev. (σ_2)	(H_o:$\sigma_1^2 = \sigma_2^2$)	(H_o:$\mu_1 = \mu_2$)
P_{max} (kN)	21.43	1.41	8.35	0.75	**5.7E-02**	**1.1E-10**[c]
Δ_{max} (mm)	55.2	2.98	20.0	4.37	1.7E-01	**2.4E-11**
E (J)	1396	198	235	37.6	**1.4E-04**	**2.0E-07**[c]
k_e (MN/m)	1.55	0.10	1.07	0.57	**9.8E-05**	**5.3E-02**[c]
μ	6.39	0.66	6.10	2.40	**1.4E-03**	7.5E-01[c]

[a] FA: (μ_1,σ_1), PA: (μ_2,σ_2).
[b] Bold values indicate statistically significant differences ($\alpha = 0.10$).
[c] T-test assuming unequal variances.

were conducted at a level of significance of 0.1 ($\alpha = 0.1$) and were possible as a result of the larger sample sizes. With respect to mean performance, fully anchored walls had statistically greater levels of P_{max}, Δ_{max}, E, and k_e. Statistically significant differences in ductility of fully and partially anchored walls were not found for SE19 tests. In addition, fully anchored walls had about 10% less ductility than partially anchored walls for SE19 and SE13 subduction zone earthquake tests (Table 5).

Drift performance. SE03 and SE13 partially anchored tests exhibited peak drifts (Δ_{peak}) 91 and 56% larger, respectively, than corresponding fully anchored tests and likewise peak-to-peak drift ($\Delta_{p\text{-}p}$) was 61 and 34% greater, respectively, for partially anchored tests (Table 4). This was not the case for SE07 and SE19, in which Δ_{peak} and $\Delta_{p\text{-}p}$ were at most approximately 10% different for fully and partially anchored walls. Therefore, although clearcut performance differences with respect to P_{max}, Δ_{max}, E, and k_e are apparent in Table 5 for fully and partially anchored walls, this was not the case for Δ_{peak} and $\Delta_{p\text{-}p}$.

For fully and partially anchored earthquake tests, SE19 caused the largest levels of Δ_{peak}, $\Delta_{p\text{-}p}$ (Table 4), total number of reverse loading cycles throughout the duration of earthquake testing, and caused the most severe damage to

Table 4. *Selected earthquake test parameters with respect to wall drift.*

	Fully anchored				Partially anchored			
	Strike-slip	Subduction zone			Strike-slip	Subduction zone		
Parameter	SE03	SE07	SE13[a]	SE19	SE03	SE07	SE13[a]	SE19
Δ_{peak} (mm)	26.8	80.5	65.9	127.4	51.2	85.4	102.5	124.4
$\Delta_{p\text{-}p}$ (mm)[b]	40.2	154.7	98.9	211.7	64.7	151.8	132.2	192.9
Total cycles[c]	57	64	78	121	51	65	81	124
T_o (s)	—	0.323	0.344	0.341	0.483	0.383	0.479	0.446
$T_{failure}$ (s)	—	0.713	0.675	0.680	0.682	0.625	0.685	0.653

[a] Conducted by Seaders et al (2009b).
[b] Sum of absolute values of maximum positive and negative peak drifts.
[c] Number of load reversing cycles during test.

Table 5. *Earthquake, monotonic, and cyclic testing backbone parameters.*

Type	Time history	Anchorage	n	P_{max} (kN)	Δ_{max} (mm)	E (J)	k_e (MN/m)	μ
Strike-slip	SE03	FA[a]	2	16.31	19.2	232	—	—
		PA	2	7.56	19.7	215[b]	0.77	3.87[b]
Subduction zone	SE07	FA[c]	2	19.69	56.1	1171	1.78	—
		PA	2	8.99	19.6	338	1.22	7.44
	SE13[d]	FA	2	23.38	59.5	744	1.51	4.04
		PA	2	8.75	22.8	250	0.78	5.97
	SE19[e]	FA	8	21.43 (7)	55.2 (5)	1396 (14)	1.55 (7)	6.39 (10)
		PA	8	8.35 (9)	20.0 (22)	235 (16)	1.07 (53)	6.10 (39)
Standardized	MT[d]	FA	2	24.34	66.3	2063	2.86	12.80
		PA	7	9.66 (15)	23.4 (16)	**238** (25)	1.34 (33)	**5.03** (25)
	CT[d]	FA	2	**22.47**	44.5	**1171**	2.01	6.82
		PA	8	**8.58** (10)	**20.8** (17)	183 (14)	**1.18** (12)	**4.92** (14)

[a] Walls did not reach ultimate loading. Average maximum observed values are reported.
[b] Reported values are based on (+) backbone curve from one test only.
[c] Walls did not reach failure. E is average of maximum observed values, ductility cannot be calculated.
[d] Conducted by Seaders et al (2009b).
[e] Seaders et al (2009b) conducted two of the eight tests for both fully and partially anchored walls.
[f] Parenthetical values are coefficients of variation (COV).
[g] Bold values indicate the parameter was within the range exhibited by the respective earthquake tests, collectively. (Parameters for the SE03 time history were excluded from the range exhibited by FA earthquake tests because the walls did not attain ultimate loading.)

fully anchored walls. This can be explained by the large accelerations in the critical region of the SE19 response spectra.

Earthquake and Standardized Testing Comparisons

This section compares performance of fully and partially anchored walls under earthquake loads with performance of walls during standard monotonic and cyclic tests conducted by Seaders et al (2009a).

Maximum load comparison. Wall capacity (P_{max}) from earthquake tests was compared with standard monotonic and cyclic tests. For fully anchored walls, P_{max} from cyclic tests fell within the range exhibited by subduction zone earthquakes, whereas P_{max} from monotonic testing provides an upper bound for earthquake tests (Table 5). This was also true for partially anchored walls; however, the range was from both the subduction zone and strike-slip earthquake tests.

Additional comparisons of P_{max} were also conducted. For fully anchored walls, average capacity from cyclic tests was about 10% closer to that of SE07 and SE19 tests than was P_{max} from monotonic tests. In addition, fully anchored SE13 earthquake tests had capacity equally similar to corresponding monotonic and cyclic tests. For partially anchored walls, average P_{max} from cyclic tests, rather than monotonic tests, was closer to all corresponding earthquake tests. In addition, P_{max} from partially anchored SE19 tests was statistically lower than P_{max} from monotonic tests and was not found to be statistically different from P_{max} of cyclic testing (Table 6).

For partially anchored walls, an additional observation with respect to P_{max} shows that the coefficient of variation from cyclic tests (10%) is less than that of monotonic tests (15%) (Table 5). Thus, among partially anchored standardized tests, cyclic tests exhibited wall capacity most similar to earthquake tests and also exhibited less variability with respect to P_{max}. Similar observations for fully anchored monotonic and cyclic tests cannot be made as a result of the smaller sample size. However, in general, results based on monotonic, cyclic, and earthquake tests suggest that partially anchored wall capacity is most accurately predicted from cyclic tests, and fully anchored wall capacity from cyclic tests is most similar to the earthquake tests.

Energy dissipation comparison. For fully anchored walls, a comparison of energy dissipation (E) shows that cyclic test values were in the range of subduction zone tests, whereas monotonic values fell above the range, thereby providing an upper limit (Tables 5 and 6). For partially anchored walls, monotonic tests yielded E within the range for subduction zone and strike-slip earthquake tests, whereas cyclic tests had E below this range.

Comparison of deflection at maximum load, initial stiffness, and wall ductility. With respect to deflection at maximum load (Δ_{max}), initial stiffness (k_e), and ductility (μ), monotonic tests of fully anchored walls exhibited values

Table 6. *Statistical tests for partially anchored walls (bold values indicate significant differences).*

	P values: MT[a] vs SE19[a]			*P* values: CT[a] vs SE19[a]		
Parameter	F-test variance test (H_o:$\sigma_1^2 = \sigma_3^2$)	T-test mean test (H_o:$\mu_1 = \mu_3$)	Ratio SE19/mono (μ_3/μ_1)	F-test variance test (H_o:$\sigma_2^2 = \sigma_3^2$)	T-test mean test (H_o:$\mu_2 = \mu_3$)	Ratio SE19/cyclic (μ_3/μ_2)
P_{max}	0.11	**0.04**	0.864	0.80	0.56	0.973
Δ_{max}	0.68	0.13	0.855	0.62	0.68	0.962
E	0.25	0.91	0.987	0.31	**0.0058**	1.28
k_e	0.55	0.33	0.799	**0.0014**	0.59[b]	0.907
μ	0.13	0.31	1.21	**0.0043**	0.22[b]	1.24

[a] MT: (μ_1,σ_1), CT: (μ_2,σ_2), SE19: (μ_3,σ_3).
[b] T-test assuming unequal variances.

that fell above the range for corresponding subduction zone earthquake tests, as shown in Table 5. Like monotonic tests, cyclic tests yielded values for k_e and μ above the range for corresponding fully anchored subduction zone earthquake tests; however, Δ_{max} from cyclic testing was below the range for fully anchored subduction zone earthquake tests. Overall, fully anchored monotonic and cyclic tests are not very representative of subduction zone earthquake tests with respect to Δ_{max}, k_e, and μ.

For partially anchored walls, monotonic testing gave Δ_{max}, k_e, and μ values above those for subduction zone and strike-slip earthquake tests with the exception of ductility (Table 5). Cyclic tests, however, exhibited values within the earthquake testing range. In general, partially anchored cyclic tests provided a good representation of corresponding earthquake tests with respect to Δ_{max}, k_e, and μ, and monotonic tests did not.

Statistical comparison. Large sample size for the partially anchored SE19 earthquake test allowed for statistical comparisons with standardized testing performance. Table 6 contains p-values for F- and T-tests with a level of significance of 0.1 ($\alpha = 0.1$) to determine if statistically significant differences in variances and means were exhibited. The p-value indicates validity of the null hypothesis, H_o, being tested (the assumption of H_o is that variance or mean values are equal) by giving the probability that random sampling would lead to a difference in variances or means as large as (or larger than) observed. A lower *p*-value indicates a higher probability of statistical difference. T-test type (assuming equal or unequal variances) was dependent on the outcome of the corresponding F-test.

For partially anchored walls, a statistical comparison of P_{max}, Δ_{max}, E, k_e, and μ from monotonic and cyclic tests with SE19 tests shows that monotonic tests yielded a statistically significant higher level for P_{max} and cyclic tests yielded a statistically significant smaller level for E (Table 6). The difference in P_{max} from monotonic and SE19 tests may be the result of the fact that monotonic tests do not incorporate load reversal, and thus fasteners do not lose embedment strength from being "loosened" in the frame. Lower E levels from cyclic tests may be a result of the cyclic protocol occurring at a much slower rate than SE19, allowing for greater stress relief and redistribution during loading, resulting in a stiffer wall, and loads occurring at smaller deflections.

Code Comparisons

Wall period. Figure 3 shows the 0.1 – 0.3 s fundamental period (T_o) estimate by FEMA 356 (Eq 1) underpredicted the actual values (using Eq 2) for fully and partially anchored walls. Average T_o for fully anchored walls was 0.336 s and slightly longer at 0.448 s for lower stiffness partially anchored walls (Table 4). Periods were elongated as a result of stiffness degradation by 105 and 48%, respectively, to 0.689 and 0.661 s for fully and partially anchored walls at maximum loading ($T_{failure}$). Fundamental periods for fully and partially anchored walls are most likely greater than those from FEMA 356 (Eq 1) for buildings because components such as partitions, cross walls, and siding contribute to building stiffness and were not incorporated into this study. Note that the partially restraining effects of the surrounding structure are an important issue here and in comparing performance of shear walls in general, especially for partially anchored walls.

Drift limit analysis. Transient drift limits per FEMA 356 are 3% for CP, 2% for LS, and 1% for IO. Among fully anchored earthquake tests, SE03 was the only one to satisfy any of these drift requirements, meeting the LS structural performance level of FEMA 356. In Seaders et al (2009b), the SE13 fully anchored earthquake test met the CP limit per FEMA 356 (Δ_{peak}/h; Table 7) and was the only fully anchored subduction zone test to meet FEMA 356 drift limit. For partially anchored walls, SE03 fulfilled the FEMA 356 collapse prevention drift

requirement. Other partially anchored earthquake tests did not satisfy any drift limits.

Moreover, Table 7 suggests that design-level earthquakes may result in similar total drift performance ($\Delta_{cumulative}$) of fully and partially anchored walls, and the peak drift (Δ_{peak}) performance of these walls may be similar for earthquakes that result in high energy demands or total wall drift.

FEMA 356 m-factor analysis. Average m-factors for earthquake tests are reported in Table 8 and compared with acceptance criteria in FEMA 356 (FEMA 2000) Table 8-4 for wood and light frame shear walls with wood structural panel sheathing or siding (aspect ratio ≤ 1). For fully and partially anchored walls, the only earthquake tests meeting the m-factor (reflecting ductility) acceptance criteria were the SE07 and SE19 tests. SE07 and SE19 tests exhibited the largest levels of cumulative drift ($\Delta_{cumulative}$), energy dissipation (E), and total energy dissipation (E_{total}) for fully and partially anchored tests (Table 8). On the contrary, for fully and partially anchored walls, SE03 and SE13 resulted in low levels of E, E_{total}, and $\Delta_{cumulative}$ causing the least observed damage among the time histories. It appears E and E_{total}, and $\Delta_{cumulative}$ can be related with the m-factor. More specifically, earthquake tests with large E, E_{total}, and $\Delta_{cumulative}$ are favorable because they met the m-factor acceptance criteria.

For SE07 fully and partially anchored tests, m-factors were essentially the same, and for SE19 fully and partially anchored tests, m-factors for partially anchored walls were 14% larger than fully anchored walls. For fully and partially anchored SE13 tests conducted by Seaders et al (2009b), partially anchored walls had m-factors 25% lower than fully anchored walls. However, the difference in m-factors of fully and partially anchored walls from SE19 and SE13 lies within the variability associated with wood materials and construction practices. In addition, small sample size for fully and partially anchored SE13 tests (two walls each) may have contributed to m-factor differences.

Table 7. *Earthquake testing results for drift analysis.*

	Fully anchored				Partially anchored			
	Strike-slip	Subduction zone			Strike-slip	Subduction zone		
Parameter	SE03	SE07	SE13[a]	SE19	SE03	SE07	SE13[a]	SE19
Δ_{peak}/h[b] (%)	1.1	3.3	2.7	5.2	2.1	3.5	4.2	5.1
$\Delta_{cumulative}$ (mm)	1002	4907	2649	5428	1323	4688	2435	4850
E_{total}[c] (J)	2177	12160	3882	9143	1496	3698	1798	3538

[a] Conducted by Seaders et al (2009b).
[b] 'h' is the story height of the building (2438 mm).
[c] Total energy dissipated during the entire duration of earthquake testing.

Table 8. *Earthquake test m-factors.*

	Fully anchored				Partially anchored			
	Strike-slip	Subduction zone			Strike-slip	Subduction zone		
Acceptance criteria (FEMA 356 Table 8-4)	SE03[a]	SE07[b]	SE13[c]	SE19	SE03	SE07	SE13[c]	SE19
CP 4.50	—	5.61	3.63	5.28	2.89	5.62	2.71	6.03
LS 3.60	—	4.21	2.72	3.96	2.16	4.22	2.03	4.52
IO 1.90	—	2.82	1.82	2.65	1.45	2.82	1.36	3.03
Parameter								
E (J)	232	1171	744	1396	215	338	250	235
E_{total}[d] (J)	2177	12163	3882	9143	1496	3698	1798	3538
$\Delta_{cumulative}$ (mm)	1002	4907	2649	5428	1323	4688	2435	4850

[a] m-factors were incalculable since tests did not reach failure (0.8 P_{max} postpeak).
[b] m-factors are based on ~0.85 P_{max} postpeak since walls did not completely fail.
[c] Conducted by Seaders et al (2009b).
[d] Total energy dissipated during the entire duration of earthquake testing.

From Seaders et al (2009a), monotonic and cyclic tests had partially anchored wall m-factors of 3.20 and 3.16, respectively, for CP. These are about 43 and 47% smaller than SE07 and SE19, respectively, and 10 and 17% larger than SE03 and SE13, respectively. Because SE13 partially anchored walls achieved failure (only one partially anchored SE03 test did), it is inconclusive whether m-factors from monotonic and cyclic tests are representative of those from partially anchored earthquake tests.

For fully anchored walls, m-factors from monotonic and cyclic tests (Seaders et al 2009a) were 6.05 and 4.20, respectively, at CP. Thus, m-factors from monotonic tests provided an upper bound to earthquake tests. The m-factor from cyclic tests is within the range for earthquake tests; however, it does not satisfy the acceptance criteria.

CONCLUSIONS

The study compared the performance of fully and partially restrained wood frame shear walls under earthquake loadings and also examined the suitability of monotonic and cyclic testing to predict seismic performance. Conclusions based on the results of this study include:

- Partially anchored subduction zone earthquake tests caused wall failure modes consistent with monotonic and cyclic tests. Fully anchored subduction zone tests caused wall failure modes consistent with cyclic tests. Fully anchored monotonic tests did not cause screw fracture or nail withdrawal and therefore did not have failure modes consistent with subduction zone earthquake tests.
- The partially anchored wall load path involved sheathing to frame fasteners along the sill plate to transmit overturning forces into the foundation, whereas fully anchored walls used hold-downs for this transfer. Thus, partially anchored walls exhibited less favorable performance in wall capacity, deflection at maximum load, energy dissipation, and initial stiffness, and less variability in observed damage severity, location, and abundance.
- For fully anchored walls, subduction zone ground motions with more cycles to maximum loading conditions and/or dissipating more energy up to these conditions resulted in smaller wall capacities. These observations did not apply to partially anchored walls because their capacity is limited by the edge breakout strength of the sheathing to sill plate fasteners.
- For fully anchored walls, with respect to monotonic and cyclic tests, subduction zone earthquake tests had capacities and energy dissipation most similar to cyclic tests rather than monotonic tests. Monotonic and cyclic tests did not provide a good representation of subduction zone earthquake tests with respect to deflection at maximum load, initial wall stiffness, and ductility. For partially anchored walls, subduction zone and strike-slip earthquake tests had capacities, deflection at maximum load, initial stiffness, and ductility most similar to cyclic tests; however, energy dissipation levels were most similar to monotonic tests.

ACKNOWLEDGMENTS

The authors acknowledge the invaluable efforts of Milo Clauson and the support provided by the Center for Wood Utilization Research at Oregon State University and the USDA (CSREES Grant).

REFERENCES

ASTM (2001) Standard test methods for cyclic (reversed) load test for shear resistance of framed walls for buildings. E 2126-02a. American Society for Testing and Materials, West Conshohocken, PA.

City of Los Angeles/UC Irvine (2001) Light frame test committee 2001, report of a testing program of light framed walls with wood-sheathed shear panels, final report to the City of Los Angeles. Dept. of Building Safety, Los Angeles, CA. 93 pp.

Cobeen K, Russell J, Dolan DJ (2004) Recommendations for earthquake resistance in the design and construction of woodframe buildings. CUREE Publication No. W-30b. Stanford University, Stanford, CA.

Dinehart DW, Shenton HW III (1998) Comparison of static and dynamic response of timber shear walls. J Struct Eng 124(6):686 – 695.

Dolan JD, Madsen B (1992) Monotonic and cyclic tests of timber shear walls. Can J Civil Eng 19(3):415 – 422.

FEMA (2000) Prestandard and commentary for the seismic rehabilitation of buildings. Rep. No. 356. Federal Emergency Management Agency, Washington, DC. 518 pp.

Filiatrault A, Foschi R (1991) Static and dynamic tests of timber shear walls fastened with nails and wood adhesive. Can J Civil Eng 18(5):749 – 755.

Gatto K, Uang CM (2003) Effects of loading protocol on the cyclic response of woodframe shearwalls. J Struct Eng 129(10):1384 – 1393.

He M, Lam F, Prion HGL (1998) Influence of cyclic test protocols on performance of wood-based shear walls. Can J Civil Eng 25(6):539 – 550.

ICC (2000) International Residential Code. International Code Council, Whittier, CA.

ISO (1998) Timber structures—Joints made with mechanical fasteners—Quasi-static reversed-cyclic test method, WG7 draft, ISO TC 165. International Organization for Standardization, Secretariat Standards Council of Canada, Ottawa, Ontario, Canada.

Karacabeyli E, Ceccotti A (1998) Nailed wood-frame shear walls for seismic Loads: test results and design considerations. Paper T207-6 in Structural Engineering World Wide. Elsevier Science, New York, NY.

Krawinkler H, Parisi F, Ibarra L, Ayoub A, Medina R (2001) Development of a testing protocol for woodframe structures, CUREE pub W-02. Richmond, CA.

Malik AM (1995) Estimating building stocks for earthquake mitigation and recovery planning. Cornell Inst for Soc and Econ Res, Cornell Univ, Ithaca, NY.

McMullin KM, Merrick DS (2000) Seismic testing of light frame shear walls. Paper No 5-4-1 *in* Proc 6th World Conf on Timber Eng, 31 July to 3 Aug, 2000, Whistler, BC.

Ni C, Karacabeyli E (2002) Capacity of shear wall segments without hold-downs. Wood Design Focus 12(2):10 – 17.

Pardoen GC, Kazanjy RP, Freund E, Hamilton CH, Larsen D, Shah N, Smith A (2000) Results from the City of Los Angeles-UC Irvine shear wall test program. Paper 1.1.1 on CD *in* Proc 6th World Conf on Timber Eng, 31 July to 3 Aug 2000, Whistler, BC.

PCA (1997) Home builder report of 1997. Portland Cement Association, Skokie, IL.

Salenikovich AJ, Dolan JD (2003a) The racking performance of shear walls with various aspect ratios, part 1, monotonic tests of fully anchored walls. Forest Prod J 53(10):65 – 73.

Salenikovich AJ, Dolan JD (2003b) The racking performance of shear walls with various aspect ratios, part 2, cyclic tests of fully anchored walls. Forest Prod J 53(11 – 12):37 – 45.

Seaders P, Gupta R, Miller TH (2009a) Monotonic and cyclic load testing of partially and fully anchored woodframe shear walls. Wood Fiber Sci 41(2):145 – 156.

Seaders P, Miller TH, Gupta R (2009b) Performance of partially and fully anchored wood-frame shear walls under earthquake loads. Forest Prod J (in press).

Somerville P, Smith N, Punyamurthula S, Sun J (1997) Development of ground motion time histories for phase 2 of the FEMA/SAC steel project, Report No. SAC/BD-97/04. SAC joint venture for the Federal Emergency Management Agency, Washington, DC.

Uang CM (2001) Loading protocol and rate of loading effects—Draft report. CUREE Caltech wood frame project, Richmond, CA.

USGS (2004a) US Geological Society. http://neic.usgs.gov/neis/eq_depot/usa/1994_01_17.html (2 Nov. 2004).

USGS (2004b) US Geological Society. http://neic.usgs.gov/neis/states/top_states.html. (2 Nov. 2004).

Yamaguchi N, Karacabeyli E, Minowa C, Kawai N, Watanabe K, Nakamura I (2000) Seismic performance of nailed wood-frame walls. Paper No 8-1-1 *in* Proc World Conf. on Timber Eng, 31 July to 3 Aug 2000, Whistler, BC.